Heliyon 10 (2024) e28471

Contents lists available at ScienceDirect

Heliyon

journal homepage: www.cell.com/heliyon

Research article

Preparation of a Carbon paste electrode with Active materials for the detection of Tetracycline

Adam Ramses Zang Akono [a,*], Niraka Blaise [b], Hambate Gomdje Valery [b,**]

[a] Department of Chemistry, Faculty of Sciences, University of Maroua, Cameroon
[b] Department of Textile and Leather Engineering, National Advanced School of Engineering of Maroua, University of Maroua, Cameroon

ARTICLE INFO

Keywords:
Electrochemical sensor
Tetracycline
Electrode
Cyclic voltammetry
Square wave voltammetry
Carbon-clay

ABSTRACT

The Electrochemical sensor based on carbon-clay paste electrode (CCPE) was constructed for sensitive determination of Tetracycline (Tc). The mineralogical composition, morphology, structure and performance of CCPE were characterized using X-ray diffraction powder, Fourier transform infrared spectroscopy (FTIR), Scanning electron microscopy (SEM) and Cyclic Voltammetry analysis. The CCPE is constituted of two types of clay having the ratio 1/1 and 2/1 characteristic of kaolinite and montmorillonite clay respectively. Its porous structure is ascribed to the presence of graphite. The CCPE exhibited a good electrocatalytic activity towards the oxidation of Tc. The electrochemical kinetics and mechanism of Tc were proposed, showing that Tc electrocatalytic oxidation reaction was controlled by diffusion process and took place in three steps. A low concentration of Tc was detected by amperometry with the linear ranges of 0.5μM–0.8 μM (R^2 = 0.98), the sensitivity was 8.01 μA/μM.cm^2, the limit of detection and quantification were 5.16x10^{-3}μM(S/N = 3) and 1.72x10^{-2}μM respectively. Thus, the proposed electrode provides a promising and prospective CCPE sensing platform for the detection of Tc in the environment.

1. Introduction

In recent years, electrochemical applications have favored the development of new composite materials that help in the design of electrochemical sensors, thus implying strong applications in various fields [1–4]. These sensors are generally made from various important materials such as carbon to detect organic compounds [5,6]. In this context, graphite is used as a basic support to modify electrodes due to its good physico-chemical properties [7,8]. It is an abundant bioavailable material obtained from vegetable residues [9] or from waste materials such as batteries [10]. Among the various adsorbents, clays and its based composites have derived a large adsorbent family endowed with the natural physicochemical properties, high specific surface area, extraordinary cation exchange capacity (CEC) and cation exchange selectivity, surface hydrophilicity, surface electronegativity, etc., and thus drawing widespread attention on environmental remediation nowadays [11,12]. The development of these new materials has been the subject of several studies in the electroanalysis of heavy metals [13,14], biomolecules [15], which open significant avenues for the design of electrochemical sensors [16]. Electrochemical sensors have interesting features such as good sensitivity, high selectivity, fast response, low cost, easy implementation and no pretreatment of the analyte [17–19]. However, other methods are also used for the detection of Tc

* Corresponding author.
** Corresponding author.
E-mail addresses: ramses5zang@yahoo.com (A.R. Zang Akono), v.hambategomdje@usms.ma (H.G. Valery).

https://doi.org/10.1016/j.heliyon.2024.e28471
Received 8 July 2023; Received in revised form 19 March 2024; Accepted 19 March 2024
Available online 21 March 2024

such as: high performance liquid chromatography [20,21], capillary electrophoresis [22], electrochemiluminescence [23,24], UV visible spectrophotometry [25–27], and high resolution mass spectrometry (HRMS) [28–30], but they are costly and not easy to implement. Electrochemical sensors have low ohmic resistance [31] and are directly applied to detect emerging pollutants in drinking water including organic molecules such as drugs [32]. The management of organic molecules such as antibiotics after use is a real problem of environmental pollution and is at the origin of the rapid growth of bacteria [33,34], hence the need to develop more reliable techniques for their detection and eradication (see Table 1).

The environmental pollution caused by antibiotics such as Tc is of concern to humanity [35,36]. Tc is a biomolecule with therapeutic properties [37–39]. Its constant use favors its release into water since there is no control before releasing it into the environment. This allows it to be stored in drinking water due to the excess of released substances creating a public health hazard [40,41], such as liver and pancreatic dysfunction in rats [42], hepatic steatosis causing liver dysfunction and severe liver failure leading to death in men [43]. The maximum limit value for Tc in milk prescribed by the European Union is 100 μg/kg [44].

The objective of this work is to design and characterize a CCPE by developing an amperometric sensor for the detection of Tc by cyclic voltammetry in aqueous solution.

2. Experimental

2.1. Material and chemical reagents

The clay material was collected in the Far North region (Cameroon), more precisely in the locality of Mokolo with the following geographic coordinates: Latitude: 10°43′59′′N, Longitude: 13°49′0.9′′E, Altitude: 799 m, Precision: ±9 m. These clays are also used by the local people for pottery. After sampling, the treatment processes were carried out according to Stockes' law as described in the literature [45]. The graphite used was taken from a recycling of battery residues, and then crushed and washed with 1 M hydrochloric acid. This purification method was inspired by previous work [10]. The paraffin oil used as a binder was purchased from the research laboratory Sisco pvt. Ltd, India. The acetic buffer solution (0.1 M, pH = 5) was prepared from sodium ethanoate and ethanoic acid solution. Acetic acid, sodium acetate and ethanol were purchased from Sigma-Aldrich. Tc was used in the pharmaceutical form.

2.2. Characterization techniques and equipment

The X-ray diffraction pattern of the natural clay powder and the carbon-clay paste electrode was recorded with a Bruker D8-Advance apparatus using Cu K alpha radiation ($\lambda = 1.54$ Å) with a diffraction angle of 2θ which varied from 5 to 50°. The morphological features of the clay and modified electrode particle surfaces were obtained using a Hitachi (Japan) S–3000H instrument. The infrared spectrum was recorded using a PERKIN-ELMER FTIR spectrometer (4000-400 cm^{-1}). Electrochemical analysis were performed using a potentiostat (model PGSTAT 100, Eco Chemie B.V., Ultrecht, Netherland) controlled by Volta lab master4 software and an electrochemical cell. The working electrode was the carbon-clay paste; the reference electrode in silver chloride and the platinum auxiliary electrode were used to detect the analyte in the solution. An Elico U 120 pH meter was used for pH measurement.

2.3. Preparation of the working electrode

The CCPE was prepared by mixing the clay (1g) thoroughly with the graphite powder (1g) using a porcelain mortar. Then, paraffin oil (3.6 mL) and ethanol (3 μL) were added into the mixture. Subsequently, this homogeneous paste was manually inserted into the cylindrical Teflon cavity (geometric surface of the working electrode with a diameter of 0.126 cm^2). Electrical contact was established with a carbon rod and the electrode was air dried for 3 h before electrochemical analysis.

2.4. Electrochemical measurement

Tetracycline was detected electrochemically by immersing the working electrode (CCPE) in an acetic buffer solution (0.1 M, pH =

Table 1
Comparison of Limit of detection of CCPE with other modified electrodes for detection of Tc.

Type of electrode	Method	Limit of Detection (LOD)	Reference
ND-MS/GCE.	DPV	2 μM	[51]
MWCNT-COOH	AdSDPV	0.36 μM	[57]
$MnWO_4$/f-CNF/GCE	CV	0.24 μM	[58]
rGO-ZnO-GCE	SWV	0.38 μM	[59]
Benzene sourced graphene-gold nanoparticle	CV	1.60×10^{-1} μM	[60]
Au-g-C_3N_4 nanocomposites	CV	0.03 μM	[61]
CME	Ads-DPCSV	0.004 μM	[64]
SbFE	SWCSV	0.15 μM	[65]
CPE-mag-MIP	SWV	0.15 μM	[66]
EPPU/GCE	SWV	1.01×10^{-1} μM	[67]
CCPE	SWV	$5.16x10^{-3}$ μM	Present work

5) containing a known concentration of tetracycline. After 5 min of analyte accumulation at the working electrode with constant stirring (500 rpm) and open circuit, electrochemical measurements were made by SWV, CV (in the potential range 0.35V and 1.15V) and EIS. As for the study of the interference effect, with the exception of the concentrations of tetracycline and glucose, which were all 2 μM, the electrochemical measurements were carried out in the same way as described above.

3. Results and discussion

3.1. X-ray diffraction analysis

The structural and mineralogical analysis using X-ray diffraction of the natural clay and CCPE were presented in Fig. 1. The patterns show almost identical peaks for both samples. The clay material consists of Smectite (5.92°), Kaolinite (12.23°), Montmorillonite (27.97°; 34.92°), and carbon probably due to the presence of organic matter in the clay, Quartz and Feldspath [46]. After modification of graphite by clay, an intense peak is observed at 26.62° characteristic of graphite in the reticular plane corresponding to the Miller index (002) [10]. The characteristic peak of Smectite at 5.92° disappears after modification. This can be explained by the interfacial interactions at the clay surface marked by the hydration of Kaolinite into halloysite whose peak is observed at 12.19° on the carbon modified by the clay.

3.2. Functional group analysis using Fourier transform infrared spectroscopy

Fig. 2 below shows the FTIR spectrums of the natural clay and CCPE. The spectrum of the natural clay shows an average band around 3500 cm^{-1} and 3600 cm^{-1}, which is characteristic of the elongation vibration of the OH-groups attributed to the kaolinite [47]. The narrow band around 3300 cm^{-1} characterizing elongation vibration of OH- groups bond and hydrophilic materials (OH-from water absorbed between the clay sheets) of 2/1 types such as montmorillonite [48]. The peak located at 3700 cm^{-1} characterized by a weak band corresponds to the vibration of the Aluminium- OH group bond of the octahedral layer of clays type1/1 such as kaolinite (Al–OH–Al). At 1650 cm^{-1}, a band is observed attributable to the OH- group of water stacked in the smectite type clay sheets. In the spectrum of the carbon paste modified by clay, an intense elongation peak corresponding to the C═C bond due to the modification of the clay by the graphite is observed between 1600 and 1645 cm^{-1}. In both spectra, very intense and medium intense bands of elongation vibration are observed between 900 and 1000 cm^{-1}, referring to the bonding of the Si–O group of quartz. The peaks located between 750 and 800 cm^{-1} is attributed to quartz. Several small bands located around 710 cm^{-1} and 520 cm^{-1} showing a deformation vibration of kaolinite and Mg–O and Mg–OH vibration corresponding to montmorillonite respectively [49].

3.3. Analysis of morphology and microstructure using SEM

Fig. 3 shows two micrographs that provide information on the morphology of the electrode surface. The natural clay in Fig. 3(a) shows a stacked layer of lamina separated each other and creating interfoliar distance. The modify graphite paste electrode depicted in Fig. 3(b) shows the same observation as above, but the difference is due to the presence of pores on the surface of the material resulting from the presence of graphite on the surface of the modified electrode. Thus, all this shows the porous character of graphite on the surface of the electrode. In both cases, the presence of shiny layers of milky white color indicates the existence of quartz and the white color subsequently indicates the existence of kaolinite. The SEM image presented in Fig. 3(c) shows a flat porous surface with a stack of graphene sheets making up the graphite.

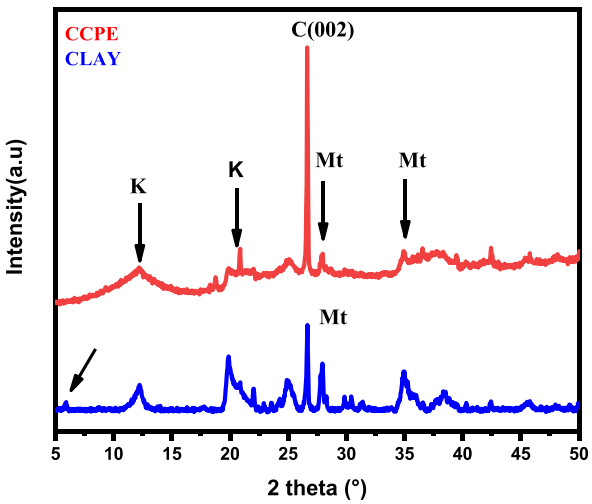

Fig. 1. X-Ray diffraction pattern of natural clay and carbon-clay paste electrode.

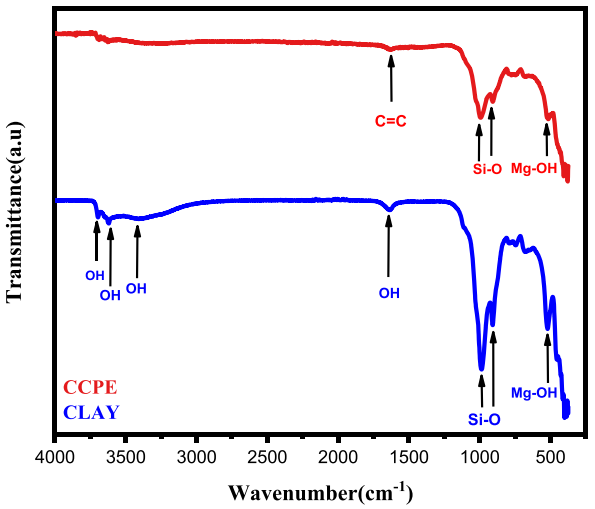

Fig. 2. FTIR spectrum of clay and carbon-clay paste electrode.

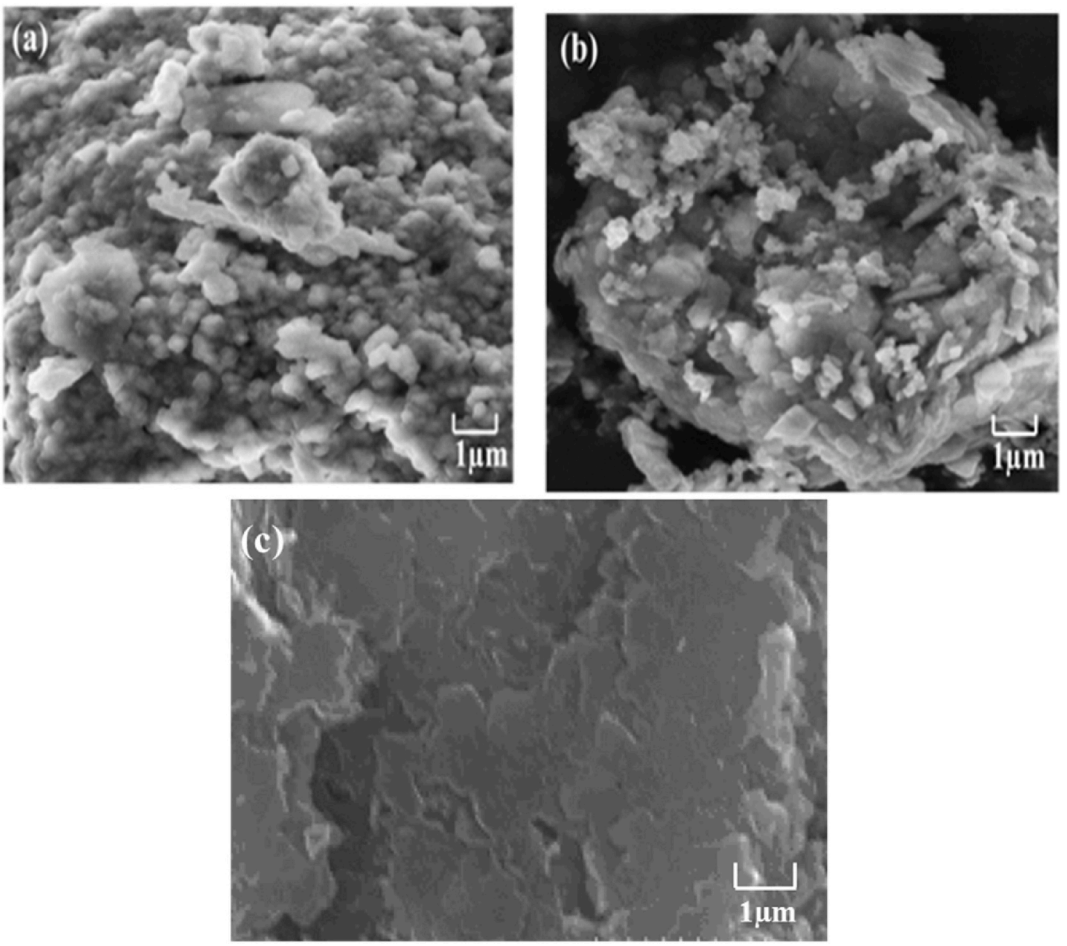

Fig. 3. SEM of: (a) clay, (b) Carbon-Clay paste, (c) Carbon Paste.

3.4. Electroanalysis of tetracycline by cyclic voltammetry

3.4.1. Electrochemical behavior of Tetracycline on a CCPE

The electrochemical behavior of Tetracycline (15 μM) on the CCPE in acetic buffer solution (0.5 M, pH = 5) at a scan rate of 50 mV/s is shown in Fig. 4. The cyclic voltammogram (CV) (a) and (b) represent the behavior of the modified electrode in the absence of Tc and in the presence of the analyte respectively. In the absence of the analyte, no peak is observed on the CV. This implies that the surface of the modified electrode does not contain any redox system and conducts the electric current perfectly in the electrolyte solution used. In the presence of Tc at a concentration equal to 15 μM, the CV shows a quasi-reversible system with an intense peak in the anodic scanning direction at $Ep_1 = 0.75V$ due to the oxidation of the alcohol function into ketone of the Tc molecule and a less intense peak due to the reduction of this same ketone function corresponding to a potential $Ep_2 = 0.41V$. This oxidation process of the alcohol function into ketone function occurs when the molecule passed through a transition state as described in the literature [50] and whose potential is perceptible in the direction of the cathodic scan at $Ep_3 = 0.64V$.

The CCPE has a good sensitivity towards Tc molecule, and the analysis of other parameters will allow a better study of the phenomenon. However, a sketch of the mechanism is proposed in the following Fig. 5.

3.4.2. Effect of pH of the electrolyte solution

Fig. 6(a) shows the CV's as a function of pH. The shifts of the potentials towards increasing values are noticeable with increasing intensities of the oxidation peaks current, which suggests that the pH has a strong influence on the oxidation reaction. The value of pH = 5 was chosen for further analysis because at this precise potential the alcohol group oxidizes with a high current peak. At higher pH values, there is a potential shift which is probably present due to the oxidation of the amine function in the Tc molecule [51].

According to Fig. 6(a), the electrochemical reaction on the surface of the modified electrode in the presence of Tc is influenced by the pH of the acetic buffer solution. This makes it possible to establish an equation between the oxidation potential as a function of pH [52].

From the straight-line, a relationship between oxidation potential and pH (Fig. 6(b)) is given by the following equation:

$$E_{pa} = 0.04pH + 0.47$$

The effect of different pH at CCPE in the presence of 15 μm Tc in 0.1 M PBS solution at scan rate of 50 mVs^{-1} as shown in Fig. 6(a), which displays the defined redox peaks, depends on the pH value (2–10) and the maximum current peak was obtained for pH = 5 [53]. The corresponding calibration line in Fig. 6(b) shows a variation in the oxidation peak potential as a function of pH, with an intense peak at pH = 5. This proves that in an acid environment there is a strong exchange of protons between the Tc and the electrode surface. Above pH = 5, the phenomenon of adsorption and ion exchange is less pronounced, but the reactions between H^+ protons and hydroxyl ions are favorable [54].

The curve $pH = f(I_{pa})$ reflects a variety of Tc species in the electrolyte solution with probably the number of protons exchanged during Tc degradation. This is in agreement with previous work describing the distribution of Tc species in aqueous solution as a function of pH showing four ionization states of Tc as a function of their respective pKa [55]. The predominant species in the electrolyte solution is the one corresponding to the highest oxidation current intensity hence the choice of pH = 5. However, this electroanalysis process of Tc is done in three steps as illustrated by the following diagram (Fig. 7):

3.4.3. Effect of scan rate

This step is crucial to better elucidate the phenomenon taking place at the surface of the modified electrode. Fig. 8(a) shows the

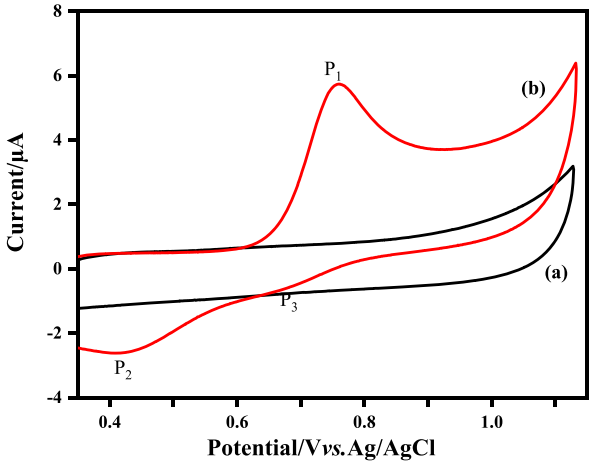

Fig. 4. CV's of the different electrodes: (a) CCPE in the absence of Tc, (b) CCPE in the presence of Tc (15 μM) in acetic buffer solution (0.1 M; pH = 5) under a scan rate of 50 mV/s.

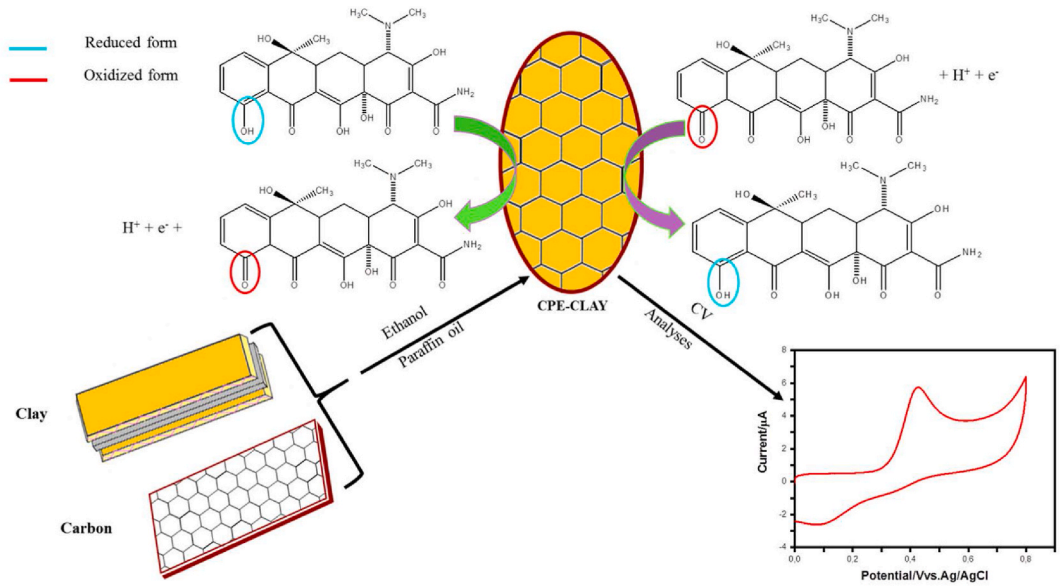

Fig. 5. Illustrative diagram of the redox mechanism of the Tc molecule at the CCPE.

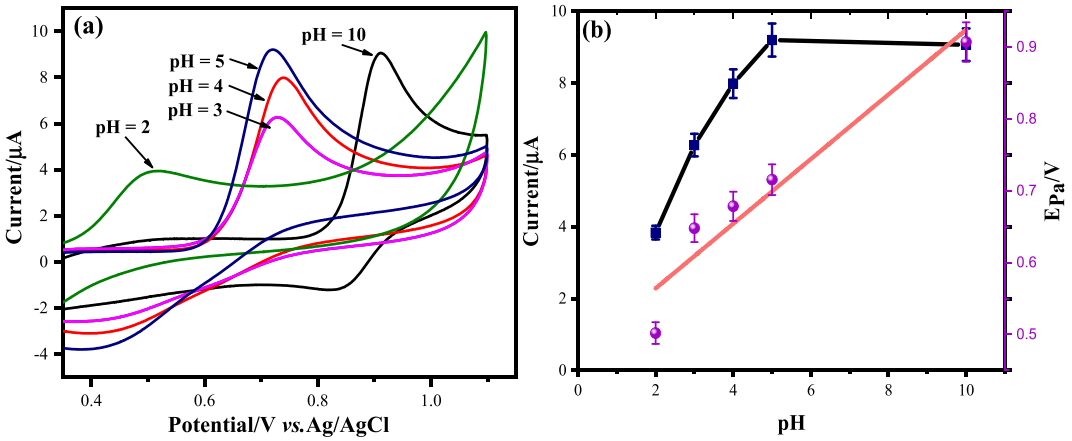

Fig. 6. CV's recorded at the CCPE electrode in the presence of Tc (15 µM) at a scan rate of 50 mV/s: (a) at different pH (2; 3; 4; 5; 10), (b) the corresponding calibration line for pH versus oxidation current and potential.

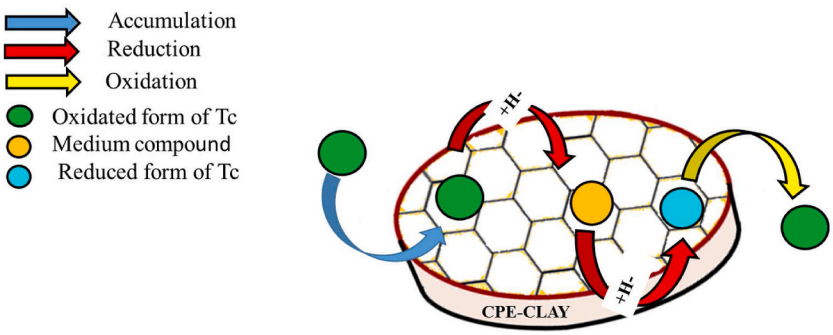

Fig. 7. Illustrative diagram of the oxidation-reduction steps of Tetracycline at the CCPE electrode.

CV's at different scan rates (30, 80, 100, 130, 150, 180 and 230 mV s^{-1}) in acetic buffer solution (0.1 M, pH = 5). The oxidation current peaks increase linearly with the square root of the scan rate as shown in Fig. 8(b) which reflects that the process is diffusion phenomenon [56].

Fig. 9(c) shows a linear function of oxidation potential *vs* scan rate $E_{pa} = f(v)$ giving a linear line equation as follows:

$$E_{pa} = 1.62 \times 10^{-4}[v] + 0.72$$

With $R^2 = 0.93$

And the intercept $E_{pa0} = 0.72$ V

The charge transfer coefficient (α_a) and the number of electrons exchanged in this process is calculated using the electrokinetic data in Fig. 9(d) and (e) following equation:

$$m = \frac{RT}{(1-\alpha_a)nF} \quad (1)$$

R, F and T are thermodynamic parameters used in working conditions, ideal gas constant, Faraday constant and absolute temperature respectively.

Thus, after calculation the found value of $\alpha_a = 0.94$ and substituting it into Eq. (1), the number of electrons exchanged during this oxidation process of Tc is $n = 0.99 \approx 1$.

3.5. Electrochemical impedance spectroscopy (EIS)

The characterization of the carbon paste electrode (CPE) and the CCPE by EIS is a very effective method of analysis which allows the electron transfer process in materials to be controlled [62]. Fig. 10 shows the Nyquist diagram in which CPE exhibits a curve similar to an affine straight line with a center of curvature having a charge transfer resistance (Rct = 1025 Ohm). This behavior reflects diffusion of the electrolyte constituents at the electrode surface, confirming the electron transfer process [63]. The CCPE curve is characterized by a much larger parabolic arc at lower frequencies than the previous curve, with a center of curvature of charge transfer resistance (Rct = 170 Ohm). This behavior shows that the CCPE electrode is favorable to redox reactions with partial diffusion during this electrochemical process. It also revealed that electron transfer is very efficient after increasing conductivity.

3.6. Electroanalysis of tetracycline by square-wave voltammetry

3.6.1. Effect of interference

Fig. 11 shows a study of the selectivity of the CCPE electrode obtained by Square-Wave Voltammetry (SWV) in an acetic buffer solution (0.1 M, pH = 5) in the presence of tetracycline and glucose, which we added to the reaction medium at equal concentration (2 μM). The electrochemical signals appear at peak potentials of −0.4V, 0.7V and 0.9V respectively for the oxidation of glucose, tetracycline and Tc excipients [66]. This voltammogram makes it possible to preserve the electrochemical identity of each molecule, which implement that the CCPE electrode detects both compounds but with a greater affinity towards glucose. It can be seen that the CCPE electrode remains selective for each molecule studied.

3.6.2. Effect of concentration

Fig. 12 shows the SWV's of Tc over a concentration range of 0.5 μM–0.8 μM in acetic buffer solution (0.1, pH = 5). The oxidation current peaks increase linearly with concentration according to the equation:

$$I = 1.01[T_C] - 0.32$$

with $R^2 = 0.98$.

The calculated limits of detection and quantification are equal to 5.16x10^{-3}μM and 1.72x10^{-2} μM respectively.

4. Conclusion

The preparation of an amperometric sensor based on carbon paste and natural clay was successfully completed. The structural, functional and electrochemical analysis showed that the modified electrode has a very good sensitivity and prompt response to the Tc molecule. It also indicates that it is less expensive than similar devices previously reported and also easy to implement. It does not require pretreatment of the analyte. Compared to the values found in the literature, the calculated values of the limit of detection and quantification are very low. Considering these results, the amperometric sensor thus designed for the detection of Tc contributes significantly to the improvement of research in electrochemistry and more particularly in environmental pollution control.

Funding statement

This research did not receive any specific grant from funding agencies in the public, commercial, or not for profit sectors.

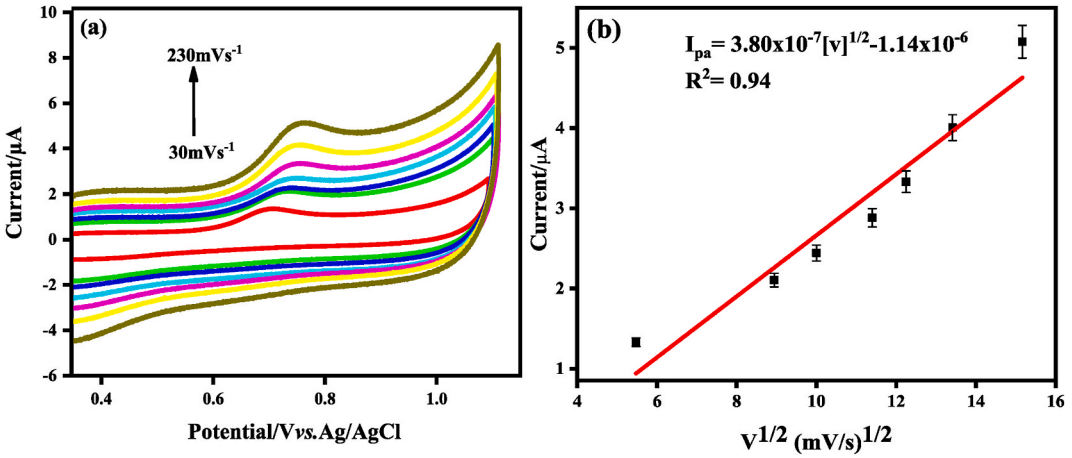

Fig. 8. CV's recorded at different scan rates by CCPE in the presence of Tc (15 µM) in acetic buffer solution (0.1 M; pH = 5).

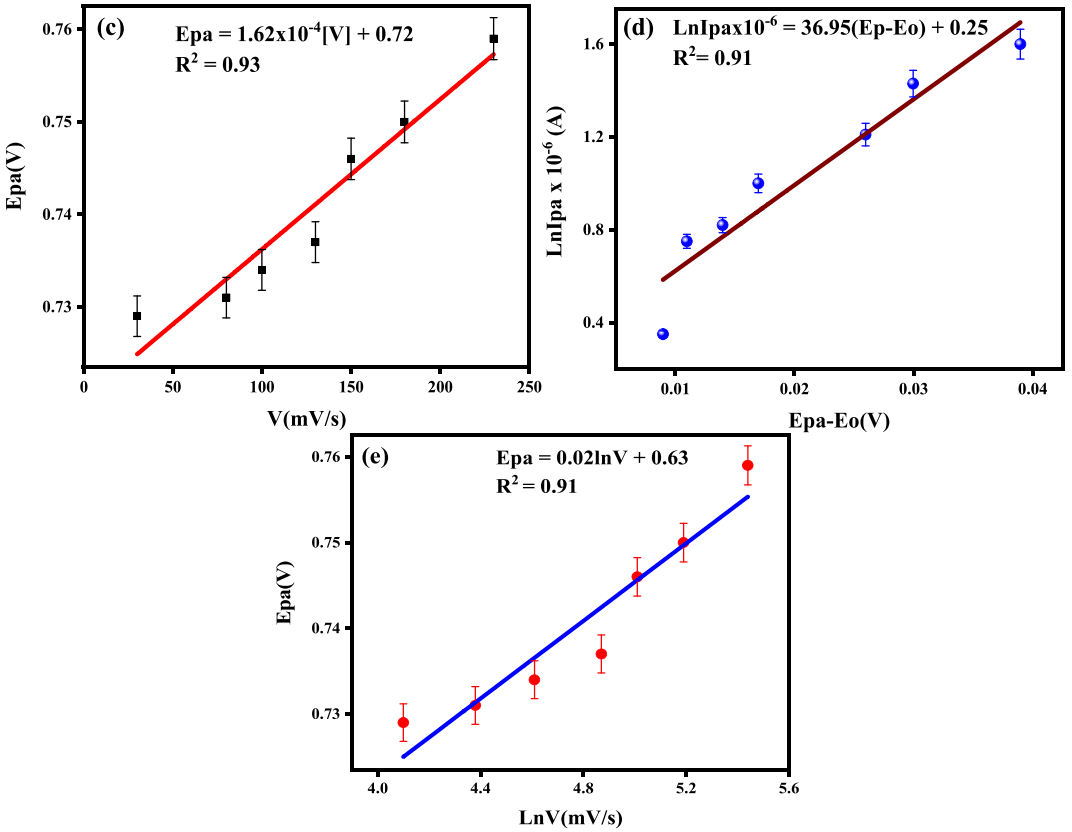

Fig. 9. (c) Experimental variation of oxidation potential as a function of scan rate; (d) experimental variation of peak current (lnI_{pa}) as a function of the difference of $E_{pa} - E_0$; (e) experimental variation of peak current (lnv) against a function of E_{pa}.

Data availability statement

Data will be made available on request.

Additional information

No additional information is available for this paper.

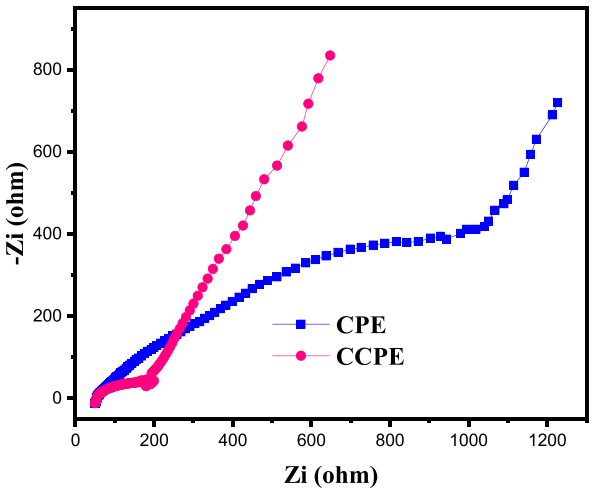

Fig. 10. Nyquist diagrams of CPE and CCPE by EIS.

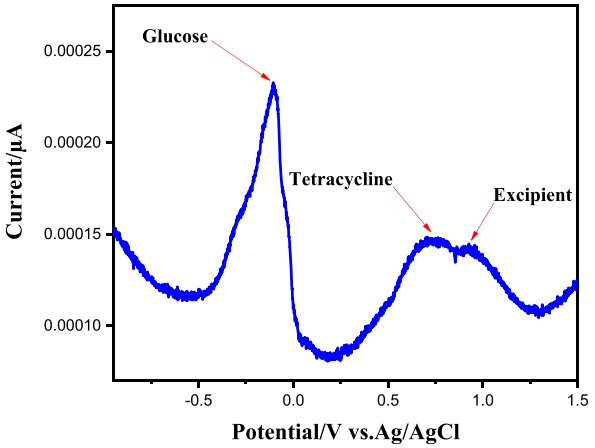

Fig. 11. Study of the interference effect by SWV.

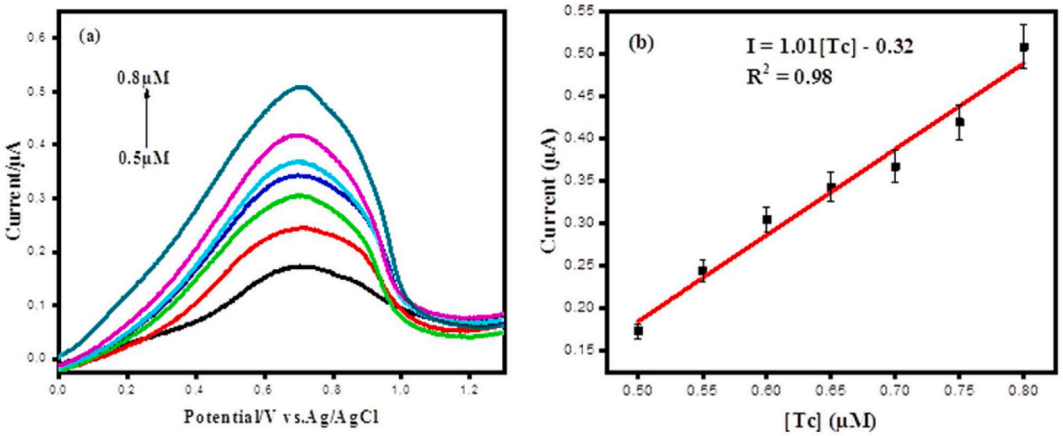

Fig. 12. SWV's recorded at different concentrations of Tc by CCPE in acetic buffer solution (0.1 M; pH = 5) (a) and its calibration curve (b).

CRediT authorship contribution statement

Adam Ramses Zang Akono: Writing – review & editing, Writing – original draft, Software, Methodology, Investigation, Data curation. **Niraka Blaise:** Writing – review & editing, Software, Methodology, Investigation. **Hambate Gomdje Valery:** Writing – review & editing, Validation, Supervision, Project administration, Methodology, Formal analysis, Conceptualization.

Declaration of competing interest

The authors declare that they have no known competing financial interests or personal relationships that could have appeared to influence the work reported in this paper.

References

[1] R.M. Cardoso, C. Kalinke, R.G. Rocha, P.L.D. Santos, D.P. Rocha, P.R. Oliveira, B.C. Janegitz, J.A. Bonacin, E.M. Richter, andA.A. Rodrigo, Additive-manufactured (3D-printed) electrochemical sensors: a critical review, Anal. Chim. Acta 1118 (2020) 73–91, https://doi.org/10.1016/j.aca.2020.03.028.

[2] A.C. Power, B. Gorey, S. Chandra, J. Chapman, Carbon nanomaterials and their application to electrochemical sensors: a review, Nanotechnol. Rev. 7 (1) (2018) 19–41, https://doi.org/10.1515/ntrev-2017-0160.

[3] X. Liu, L. Huang, K. Qian, Nanomaterial-based electrochemical sensors: mechanism, preparation, and application in Biomedicine, Adv. NanoBiomed Res. 1 (6) (2021) 2000104, https://doi.org/10.1002/anbr.202000104.

[4] J.D.T. Bakary, B. Niraka, V.G. Hambate, Investigation of the photoactivation effect of TiO2 onto carbon-clay paste electrode by cyclic voltammetry analysis, Heliyon 9 (2) (2023) e13474, https://doi.org/10.1016/j.heliyon.2023.e13474.

[5] C.M. Chou, Y.D. Dai, C. Yuan, Y.H. Shen, Preparation of an electrochemical sensor utilizing graphene-like biochar for the detection of tetracycline, Environ. Res. 236 (2) (2023) 116785, https://doi.org/10.1016/j.envres.2023.116785.

[6] A. Kareem, K. Thenmozhi, S. Hari, V.K. Ponnusamy, S. Senthilkumar, Metal-free carbon-based anode for electrochemical degradation of tetracycline and metronidazole in wastewater, Chemosphere 351 (2024) 141219, https://doi.org/10.1016/j.chemosphere.2024.141219.

[7] D. Gravis, S. Moisan, F. Poncin-Epaillard, Characterization of surface physico-chemistry and morphology of plasma-sized carbon fiber, Thin Solid Films 721 (2021) 138555, https://doi.org/10.1016/j.tsf.2021.138555.

[8] L.F. Aval, M. Ghoranneviss, G.B. Pour, High-performance supercapacitors based on the carbon nanotubes, graphene and graphite nanoparticles electrodes, Heliyon 4 (11) (2018) e00862, https://doi.org/10.1016/j.heliyon.2018.e00862.

[9] L. Zhang, F. Deng, X. Chen, Z. Guo, H. Liu, X. Xing, Z. Zhang, Microstructure graphitization evolution and multi-scale, multi-mechanism synergistic enhancement of ultra-high strength carbon-graphite materials, Diam. Relat. Mater. 128 (2022) 109271, https://doi.org/10.1016/j.diamond.2022.109271.

[10] R.T. Doumbi, G.B. Noumi, Domga, « Dip coating deposition of manganese oxide nanoparticles on graphite by sol gel technique for the indirect electrochemical oxidation of methyl orange dye: parameter's optimization using box-behnken design, Case Stud. Chem. Environ. Eng. 3 (2021) 100068, https://doi.org/10.1016/j.cscee.2020.100068.

[11] T. Zhang, W. Wang, Y. Zhao, H. Bai, T. Wen, S. Kang, G. Song, S. Song, Removal of heavy metals and dyes by clay-based adsorbents: from natural clays to 1D and 2D nano-composites, Chem. Eng. J. 420 (2021) 127574, https://doi.org/10.1016/j.cej.2020.127574.

[12] S. Gu, X. Kang, L. Wang, E. Lichtfouse, C. Wang, Clay mineral adsorbents for heavy metal removal from wastewater: a review, Environ. Chem. Lett. 17 (2) (2019) 629–654, https://doi.org/10.1007/s10311-018-0813-9.

[13] B. Niraka, V.G. Hambate, R. Maallah, M. Oubaouz, J.D.T. Bakary, E.A. Ofudje, A. Chtaini, Simultaneous electrochemical detection of Pb and Cd by carbon paste electrodes modified by activated clay, J. Anal. Methods Chem. 2022 (2022) e6900839, https://doi.org/10.1155/2022/6900839.

[14] J. Estrada-Aldrete, J.M. Hernández-López, A.M. García-León, J.M. Peralta-Hernández, F.J. Cerino-Córdova, Electroanalytical determination of heavy metals in aqueous solutions by using a carbon paste electrode modified with spent coffee grounds, J. Electroanal. Chem. 857 (2020) 113663, https://doi.org/10.10116/j.jelechem.2019.113663.

[15] N.P. Shetti, D.S. Nayak, K.R. Reddy, T.M. Aminabhvi, Chapter 10 - graphene–clay-based Hybrid Nanostructures for electrochemical sensors and biosensors, in: inGraphene-Based Electrochemical Sensors for Biomolecules, A. Pandikumar and P. Rameshkumar, Elsevier, 2019, pp. 235–274, https://doi.org/10.1016/B978-0-12-815394-9.00010-8.

[16] P.R. Vernekar, N.P. Shetti, M.M. Shanbhag, S.J. Malode, R.S. Malladi, K.R. Reddy, Novel layered structured bentonite clay-based electrodes for electrochemical sensorapplications, Microchem. J. 159 (2020) 105441, https://doi.org/10.1016/j.microc.2020.105441.

[17] H. Sohrabi, O. Arbabzadeh, P. Khaaki, A. Khataee, M.R. Majidi, Y. Orooji, Patulin and Trichothecene: characteristics, occurrence, toxic effects and detection capabilities via clinical, analytical and nanostructured electrochemical sensing/biosensing assays in foodstuffs, Crit. Rev. Food Sci. Nutr. 62 (20) (2022) 5540–5568, https://doi.org/10.1080/10408398.2021.1887077.

[18] B. Debnath, M. Majumdar, M. Bhowmik, K.L. Bhowmik, A. Debnath, D.N. Roy, The effective adsorption of tetracycline onto zirconia nanoparticles synthesized by novel microbial green technology, J. Environ. Manag. 261 (2020) 110235, https://doi.org/10.1016/j.jenvman.2020.110235.

[19] Q. Liao, H. Rong, M. Zhao, H. Luo, Z. Chu, R. Wang, Interaction between tetracycline and microorganisms during wastewater treatment: a review, Sci. Total Environ. 757 (2021) 143981, https://doi.org/10.1016/j.scitotenv.2020.143981.

[20] J.Y. Pailler, A. Krein, L. Pfister, L. Hoffmann, C. Guignard, Solid phase extraction coupled to liquid chromatography-tandem mass spectrometry analysis of sulfonamides, tetracyclines, analgesics and hormones in surface water and wastewater in Luxembourg, Sci. Total Environ. 407 (16) (2009) 4736–4743, https://doi.org/10.1016/j.scitotenv.2009.04.042.

[21] B. Vuran, H.I. Ulusoy, G. Sarp, E. Yilmaz, U. Morgül, A. Kabir, A. Tartaglia, M. Locatelli, M. Soylak, « Determination of chloramphenicol and tetracycline residues in milk samples by means of nanofiber coated magnetic particles prior to high-performance liquid chromatography-diode array detection, Talanta 230 (2021) 122307, https://doi.org/10.1016/j.talanta.2021.122307.

[22] D. Moreno-González, M. Krulišová, L. Gámiz-Gracia, A.M. García-Campaña, Determination of tetracyclines in human urine samples by capillary electrophoresis in combination with field amplified sample injection, Electrophoresis 39 (4) (2018) 608–615, https://doi.org/10.1002/elps.201700288.

[23] L. Jin, J. Qiao, J. Chen, N. Xu, M. Wu, Combination of area controllable sensing surface and bipolar electrode-electrochemiluminescence approach for the detection of tetracycline, Talanta 208 (2020) 120404, https://doi.org/10.1016/j.talanta.2019.120404.

[24] R. Xu, Z. Shen, Y. Xiang, J. Huang, G. Wang, F. Yang, J. Sun, J. Han, W. Liu, X. Duan, L. Zhang, J. Zhao, X. Sun, Y. Guo, Portable electrochemiluminescence detection system based on silicon photomultiplier single photon detector and aptasensor for the detection of tetracycline in milk, Biosens. Bioelectron. 220 (2023) 114785, https://doi.org/10.1016/j.bios.2022.114785.

[25] J. Chapman, R. Orrell-Trigg, K.Y. Kwoon, V.K. Truong, D. Cozzolino, A high-throughput and machine learning resistance monitoring system to determine the point of resistancefor Escherichia coli with tetracycline:Combining UV-visible spectrophotometry with principal component analysis, Biotechnol. Bioeng. 118 (4) (2021) 1511–1519, https://doi.org/10.1002/bit.27664.

[26] A.M. Huerta-Flores, I. Juárez-Ramírez, L.M. Torres-Martínez, J.E. Carrera-Crespo, T. Gómez-Bustamante, O. Sarabia-Ramos, Synthesis of $AMoO_4$ (A = Ca, Sr, Ba) photocatalysts and their potential application for hydrogen evolution and the degradation of tetracycline in water, J. Photochem. Photobiol. Chem. 356 (2018) 29–37, https://doi.org/10.1016/j.jphotochem.2017.12.029.

[27] Y. Feng, D. Zhong, H. Miao, X. Yang, « Carbon dots derived from rose flowers for tetracyclinesensing, Talanta 140 (2015) 128–133, https://doi.org/10.1016/j.talanta.2015.03.038.

[28] M. Solliec, A. Roy-Lachapelle, S. Sauvé, Quantitative performance of liquid chromatography coupled to Q-Exactive high resolution mass spectrometry (HRMS) for the analysis of tetracyclines in a complex matrix, Anal. Chim. Acta 853 (2015) 415–424, https://doi.org/10.1016/j.aca.2014.10.037.

[29] M. Llorca, S. Rodríguez-Mozaz, O. Couillerot, K. Panigoni, J.d. Gunzburg, S. Bayer, R. Czaja, D. Barceló, « Identification of new transformation products during enzymatic treatment of tetracycline and erythromycin antibiotics at laboratory scale by an on-line turbulent flow liquid-chromatography coupled to a high resolution mass spectrometer LTQ-Orbitrap, Chemosphere 119 (2015) 90–98, https://doi.org/10.1016/j.chemosphere.2014.05.072.

[30] K. Sun, Q. Huang, S. Li, Transformation and toxicity evaluation of tetracycline in humic acid solution by laccase coupled with 1-hydroxybenzotriazole, J. Hazard Mater. 331 (2017) 182–188, https://doi.org/10.1016/j.jhazmat.2017.02.058.

[31] N.A. Zambianco, T.A. Silva, H. Zanin, O. Fatibello-Filho, B.C. Janegitz, Novel electrochemical sensor based on nanodiamonds and manioc starch for detection of diquat in environmental samples, Diam. Relat. Mater. 98 (2019) 107512, https://doi.org/10.1016/j.diamond.2019.107512.

[32] B. Zanfrognini, L. Pigani, C. Zanardi, Recent advances in the direct electrochemical detection of drugs of abuse, J. Solid State Electrochem. 24 (11) (2020) 2603–2616, https://doi.org/10.1007/s10008-020-04686-z.

[33] A.A. Mohammed, S.L. Kareem, Adsorption of tetracycline fom wastewater by using Pistachio shell coated with ZnO nanoparticles: equilibrium, kinetic and isotherm studies, Alex. Eng. J. 58 (3) (2019) 917–928, https://doi.org/10.1016/j.aej.2019.08.006.

[34] Q. Liao, H. Rong, M. Zhao, H. Luo, Z. Chu, R. Wang, Interaction between tetracycline and microorganisms during wastewater treatment: a review, Sci. Total Environ. 757 (2021) 143981, https://doi.org/10.1016/j.scitotenv.2020.143981.

[35] H. Liu, G. Xu, G. Li, Preparation of porous biochar based on pharmaceutical sludge activated by NaOH and its application in the adsorption of tetracycline, J. Colloid Interface Sci. 587 (2021) 271–278, https://doi.org/10.1016/j.jcis.2020.12.014.

[36] J. Wei, Y. Liu, J. Li, Y. Zhu, H. Yu, Y. Peng, Adsorption and co-adsorption of tetracycline and doxycycline by one-step synthesized iron loaded sludge biochar, Chemosphere 236 (2019) 124254, https://doi.org/10.1016/j.chemosphere.2019.06.224.

[37] M. Sodhi, M. Etminan, « therapeutic potential for tetracyclines in the treatment of COVID-19, Pharmacotherapy 40 (5) (2020) 487–488, https://doi.org/10.1002/phar.2395.

[38] M.L. Nelson, S.B. Levy, The history of the tetracyclines, Ann. N. Y. Acad. Sci. 1241 (1) (2011) 17–32, https://doi.org/10.1111/j.1749-6632.2011.06354.x.

[39] M.O. Griffin, E. Fricovsky, G. Ceballos, F. Villarreal, « Tetracyclines: a pleitropic family of compounds with promising therapeutic properties. Review of the literature, Am. J. Physiol. Cell Physiol. 299 (3) (2010) C539–C548, https://doi.org/10.1152/ajpcell.00047.2010.

[40] J. Wyszkowska, A. Borowik, J. Kucharski, The role of grass compost and Zea Mays in Alleviating toxic effects of tetracycline on the soil bacteria community, Int. J. Environ. Res. Publ. Health 19 (12) (2022), https://doi.org/10.3390/ijerph19127357.

[41] S.A.D.A. Fernandes, A.P.A. Magnavita, S.P.B. Ferrao, Daily ingestion of tetracycline residue present in pasteurized milk: a public health problem, Environ. Sci. Pollut. Res. 21 (5) (2014) 3427–3434, https://doi.org/10.1007/s11356-013-2286-5.

[42] M.B. Shabana, H.M. Ibrahim, S.E.M. Khadre, M.G. Elemam, Influence of rifampicin and tetracycline administration on some biochemical and histological parameters in albino rats, J. Basic Appl. Zool. 65 (5) (2012) 299–308, https://doi.org/10.1016/j.jobaz.2012.10.009.

[43] M.A. Shaker, W.H. Alshitari, M.T. Basha, N.A. Aly, M. Asim, H.M. Albishri, S.A. Bhawani, A.A. Yakout, «Synergetic impact of copper nanoparticles and polyaniline reinforced graphene oxide nanocomposite on the sequestration of tetracycline antibiotic from milk and wastewaters samples, Mater. Today Commun. 38 (2024) 107869, https://doi.org/10.1016/j.mtcomm.2023.107869.

[44] G. Islas, J.A. Rodriguez, I. Perez-Silva, J.M. Miranda, I.S. Ibarra, Solid-Phase extraction and large-volume sample stacking-capillary electrophoresis for determination of tetracycline residues in milk, J. Anal. Methods Chem. 2018 (2018) e5394527, https://doi.org/10.1155/2018/5394527.

[45] L.A. Shah, M.G.S. Valenzuela, M. Farooq, S.A. Khattak, F.R.V. Díaz, «Influence of preparation methods on textural properties of purified bentonite, Appl. Clay Sci. 162 (2018) 155–164, https://doi.org/10.1016/j.clay.2018.06.001.

[46] R. Danga, P. Abba, C. Tsamo, B. Loura, « Synthesis of clay-biochar composite for glyphosate removal from aqueous solution, Heliyon 8 (3) (2022) e09112, https://doi.org/10.1016/j.heliyon.2022.e09112.

[47] Y.E. Bouabi, A. Loudiki, M. Matrouf, R. Matrou, R.A. Akbour, F. Laghrib, A. Farahi, M. Bakasse, S. Saqrane, S. Lahrich, M.A.E. Mhammedi, Clay-based graphite sensor for electrochemical determination of paranitrophenol in water samples, Case Stud. Chem. Environ. Eng. 6 (2022) 100225, https://doi.org/10.1016/j.cscee.2022.100225.

[48] O. Bouras, J.C. Bollinger, M. Baudu, H. Khalaf, Adsorption of diuron and its degradation products from aqueous solution by surfactant-modified pillared clays, Appl. Clay Sci. 37 (3) (2007) 240–250, https://doi.org/10.1016/j.clay.2007.01.009.

[49] Y. Dehmani, A. Ed-Dra, O. Zennouhi, A. Bouymajane, F.R. Filali, L. Nassiri, S. Abouarnadasse, Chemical characterization and adsorption of oil mill wastewater on Moroccan clay in order to be used in the agricultural field, Heliyon 6 (1) (2020) e03164, https://doi.org/10.1016/j.heliyon.2020.e03164.

[50] V. Khakyzadeh, S. Sediqi, The electro-oxidation of primary alcohols via a coral-shaped cobalt metal–organic framework modified graphite electrode in neutral media, Sci. Rep. 12 (1) (2022), https://doi.org/10.1038/s41598-022-12200-w.

[51] W.S. Fernandes-Junior, L.F. Zaccarin, G.G. Oliveira, Electrochemical sensor based on nanodiamonds and manioc starch for detection of tetracycline, J. Sens. 2021 (2021) e6622612, https://doi.org/10.1155/2021/6622612.

[52] V.A. Kothandan, S. Mani, S. Chen, S.H. Chen, Ultrasonic-assisted synthesis of nickel tungstate nanoparticles on poly (3,4-ethylene dioxythiophene):poly (4-styrene sulfonate) for the effective electrochemical detection of caffeic acid, Mater. Today Commun. 26 (2021) 101833, https://doi.org/10.1016/j.mtcomm.2020.101833.

[53] M. Sakthivel, M. Sivakumar, S.M. Chen, Y.S. Hou, V. Veeramani, R. Madhu, N. Miyamoto, A Facile synthesis of Cd(OH) 2-rGO nanocomposites for the practical electrochemical detection of acetaminophen, Electroanalysis 28 (2016) 1–8, https://doi.org/10.1002/elan.201600351.

[54] V. Veeraman, M. Sivakumar, S.M. Chen, R. Madhu, H.R. Alamri, Z.A. Alothman, M.S.A. Hossain, C.K. Chen, Y. Yamauchi, N. Miyamoto, K.C.W. Wu, Lignocellulosic biomass-derived, graphene sheet-like porous activated carbon for electrochemicalsupercapacitor and catechin sensing, RSC Adv. 7 (2017) 45668–45675, https://doi.org/10.1039/C7RA07810B.

[55] A. Balakrishnan, M. Chinthala, R.K. Polagani, D.V.N. Vo, Removal of tetracycline from wastewater using g-C_3N_4 based photocatalysts: a review, Environ. Res. 216 (3) (2023) 114660, https://doi.org/10.1016/j.envres.2022.114660.

[56] M. Gashu, A. Kassa, M. Tefera, M. Amare, B.A. Aragaw, Sensitive and selective electrochemical determination of doxycycline in pharmaceutical formulations using poly(dipicrylamine) modified glassy carbon electrode, Sens. Bio-Sens. Res. 37 (2022) 100507, https://doi.org/10.1016/j.sbsr.2022.100507.

[57] A. Wong, M. Scontri, E.M. Materon, M.R.V. Lanza, M.D.P.T. Sotomayor, Development and application of an electrochemical sensor modified with multi-walled carbon nanotubes and graphene oxide for the sensitive and selective detection of tetracycline, J. Electroanal. Chem. 757 (2015) 250–257, https://doi.org/10.1016/j.jelechem.2015.10.001.

[58] R. Ramkumar, G. Dhakal, J.J. Shim, W.K. Kim, Differential pulse voltammetric sensor for tetracycline using manganese tungstate nanowafers and functionalized carbon nanofiber modified electrode, Kor. J. Chem. Eng. 39 (8) (2022) 2192–2200, https://doi.org/10.1007/s11814-021-1055-2.

[59] A. Đurović, Z. Stojanović, Z. Bytešníková, Reduced graphene oxide/ZnO nanocomposite modified electrode for the detection of tetracycline, J. Mater. Sci. 57 (9) (2022) 5533–5551, https://doi.org/10.1007/s10853-022-06926-1.

[60] A.O. Osikoya, P.P. Govender, Electrochemical detection of tetracycline on highly sensitive benzene sourced CVD graphene-gold nanoparticles nanointerfaces, Electroanalysis 33 (2) (2021) 412–420, https://doi.org/10.1002/elan.202060230.

[61] H. Guo, Y. Su, Y. Shen, Y. Long, W. Li, In situ decoration of Au nanoparticles on carbon nitride using a single-source precursor and its application for the detection of tetracycline, J. Colloid Interface Sci. 536 (2019) 646–654, https://doi.org/10.1016/j.jcis.2018.10.104.

[62] A. Wong, A.C. Riojas, A.M.B. Moncada, M.D.P.T. Sotomayor, A new electrochemical platform based on carbon black paste electrode modified with α-cyclodextrin and hierarchical porous carbon used for the simultaneous determination of dipyrone and codeine, Microchem. J. 164 (2021) 106032, https://doi.org/10.1016/j.microc.2021.106032.

[63] A. Andy, C. Riojas, A. Wong, G.A. Planes, M.D.P.T. Sotomayor, A.L.R. Toro, A.M.B. Moncada, Development of a new electrochemical sensor based on silver sulfide nanoparticles and hierarchical porous carbon modified carbon paste electrode for determination of cyanide in river water samples, Sensor. Actuator. B Chem. 287 (2019) 544–550, https://doi.org/10.1016/j.snb.2019.02.053.

[64] Z.R. Dizavandi, A. Aliakbar, M. Sheykhan, A novel Pb-poly aminophenol glassy carbon electrode for determination of tetracycline by adsorptive differential pulse cathodic stripping voltammetry, Electrochim. Acta 227 (2017) 345–356, https://doi.org/10.1016/j.electacta.2016.12.167.
[65] G. Krepper, G.D. Pierini, M.F. Pistonesi, M.S. Di Nezio, In-situ antimony film electrode for the determination of tetracyclines in Argentinean honey samples, Sensors andActuators B: Chemical. 241 (2017) 560–566, https://doi.org/10.1016/j.snb.2016.10.125.
[66] S. Zeb, A. Wong, S. Khan, S. Hussain, M.D.P.T. Sotomayor, Using magnetic nanoparticles/MIP-based electrochemical sensor for quantification of tetracycline in milk samples, J. Electroanal. Chem. 900 (2021) 115713, https://doi.org/10.1016/j.jelechem.2021.115713.
[67] M. Gashu, B.A. Aragaw, M. Tefera, Voltammetric determination of oxytetracycline in milk and pharmaceuticals samples using polyurea modified glassy carbon electrode, J. Food Compos. Anal. 117 (2023) 105128, https://doi.org/10.1016/j.jfca.2023.105128.